KLAM_21 DRAINAGE WIND MODELLING OF WINTERTIME AIR POLLUTION EVENTS IN CHRISTCHURCH, NEW ZEALAND

Meinolf Kossmann and Uwe Sievers

Deutscher Wetterdienst, Offenbach am Main, Germany. E-mail : *meinolf.kossmann@dwd.de*

Abstract: The cold air drainage model KLAM_21 is used to simulate the surface wind field during winter smog nights in Christchurch, New Zealand. Comparison of model results with detailed observations of the CAPS2000 field campaign indicates that the complex flow field of interacting local and regional winds is captured well by the model.

Keywords: *air pollution, complex terrain, cold air drainage, land breeze, country breeze, flow convergence, PM10*

1. INTRODUCTION

Detailed knowledge of the depth and intensity of nocturnal drainage wind systems is required for many aspects of environmental consultancy, such as the assessment of urban ventilation or frost risk during calm synoptic conditions. Drainage winds are often superimposed on regional wind systems or other thermally induced local wind systems, e.g. land breezes or country breezes. The Environment and Climate Consultancy Department of the German national weather service (DWD) developed the cold air drainage model KLAM_21 (Sievers, 2005) as a fast and easy-to-use tool to estimate the behaviour and impact of these nocturnal wind systems with high spatial and temporal resolution under varying environmental conditions.

In this study the cold air drainage model KLAM_21 is used to simulate the nocturnal surface wind field during winter smog nights in the area of Christchurch, a city of about 400000 inhabitants, located on the east coast of New Zealand’s South Island. Model results are compared to observations taken during the CAPS2000 field campaign (Kossmann and Sturman, 2004; Corsmeier et al., 2006).

2. THE COLD AIR DRAINAGE MODEL KLAM_21

The model calculates depth and velocity of a surface based stable layer that evolves from a neutrally stratified, dry atmosphere during nighttime. The prediction of the velocity and direction of the cold air drainage is based on a vertically averaged momentum tendency equation. Temporal changes in the total heat deficit E of the stably stratified cold air layer are calculated from a prescribed constant local heat loss rate P (depends only on surface type, see Table 1) and horizontal advection:

$$\frac{\partial E}{\partial t} = P - \nabla_h \cdot \rho_0 \, c_p \, H \, \langle \vec{v}_h \; T' \rangle \qquad (1)$$

Brackets $\langle ... \rangle$ indicate vertical averaging from the height of the terrain surface above sea level h_0 to $h_0 + H$ the top of the stably stratified cold air layer of depth H. $\vec{v}_h$ is the horizontal wind vector, c_p is the heat capacity of the air at constant pressure, and ρ_0 is the mean air density in the cold air layer. The air temperature disturbance T' in the cold air layer is given by a universal parabolic profile (Figure 1) using the scaling parameters ΔT_0 (=3 K) and H_0 (=10 m):

$$T'(x,y,z) = \underbrace{\Delta T_0 \left(\frac{H(x,y)}{H_0} \right)^{1/2}}_{\Delta T(H)} \underbrace{\left(\frac{h_0(x,y) + H(x,y) - z}{H(x,y)} \right)^2}_{f(H,z)} \qquad (2)$$

The total depth of the stably stratified cold air layer is calculated diagnostically every model time step from the total heat deficit E:

$$H(x,y) = H_0 \left(\frac{E(x,y)}{c_p \, \langle f \rangle \, H_0 \, \Delta T_0} \right)^{2/3} \qquad \text{where} \quad \langle f \rangle = 1/3 \qquad (3)$$

Observations indicate that only the lower part of the stably stratified cold air layer of depth $H_{eff}=\beta H$ contributes effectively to the forcing of drainage winds, while weak return circulations or regional winds usually dominate aloft between H_{eff} and H, where horizontal temperature gradients are less pronounced. Sievers (2005) applied energy considerations to derive $\beta=5/12$. KLAM_21 approximates the vertical drainage wind profile $v_h(z)$ by a universal triangular wind profile with a wind speed maximum $v_{h\,max}=2<v_h>$ at the height $0.25H_{eff}$ and wind speed decaying linearly from this value to zero wind at the surface and at H (Figure 1). Neglecting Coriolis effects and assuming the advection of momentum is balanced by a dynamic pressure perturbation, the vertically averaged tendency equation of horizontal momentum is given by:

$$\underbrace{\frac{\partial\langle\vec{v}_h\rangle}{\partial t}}_{I} = \underbrace{-\frac{g\,\Delta T\,\langle f\rangle}{T_0}\mathbf{T}^2\cdot\nabla_h\left(h_0+\beta H\right)}_{II} + \underbrace{\overbrace{l\left|\langle\vec{v}_t\rangle\right|\mathbf{D}\cdot\langle\vec{v}_h\rangle}^{a} - \overbrace{\frac{1}{H}c_*\langle\vec{v}_h\rangle\left|\langle\vec{v}_t\rangle\right|}^{b}}_{III} + \underbrace{REG}_{IV} \qquad (4)$$

with the wind vector tangential to the surface $\vec{v}_t=\mathbf{T}^{-1}\cdot\vec{v}_h$. Local temporal changes in $\langle\vec{v}_h\rangle$ (term I) result from imbalances between effective gravitational forcing (term II), friction (term III), and the effects of a regional wind (term IV). The friction term consists of surface and canopy friction (term IIIb) and the effects of horizontal diffusion (term IIIa). T_0 represents a typical mean temperature in the cold air layer and c_* is the friction coefficient which depends on H_{eff}. In forested and urban areas c_* is also a function of canopy height and the leaf/wall area index. The mixing length l is set to the typical nocturnal value $l=1\ m$. The projection operator **T** from the tangential to the horizontal plane and the differential operator **D** are:

$$\mathbf{T}=\begin{pmatrix} 1/\sqrt{1+\left(\frac{\partial h_0}{\partial x}\right)^2} & 0 \\ 0 & 1/\sqrt{1+\left(\frac{\partial h_0}{\partial y}\right)^2}\end{pmatrix} \quad \text{and} \quad \mathbf{D}=\begin{pmatrix} \frac{\partial}{\partial y^2} & 0 \\ 0 & \frac{1}{\partial x^2}\end{pmatrix} \qquad (5)$$

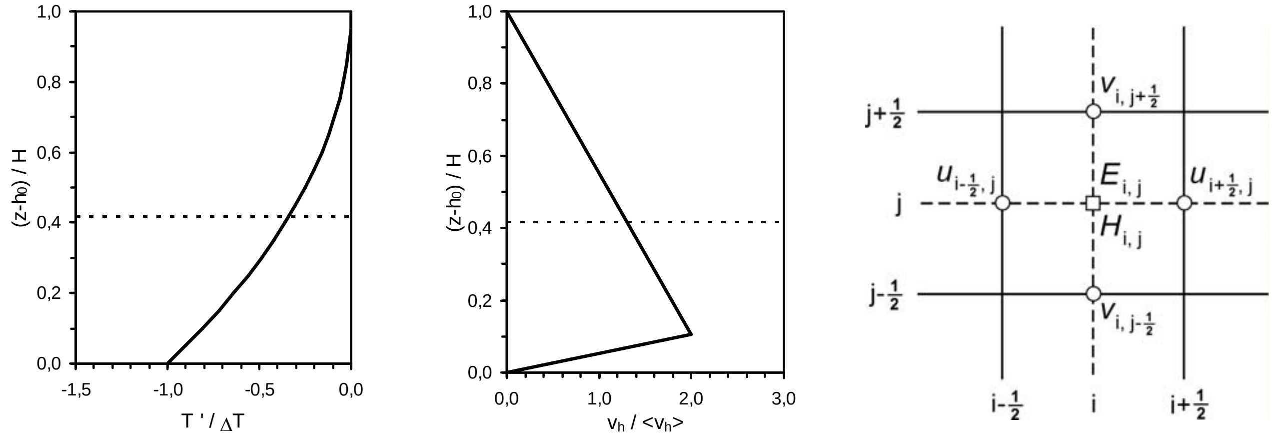

Figure 1: Schematic representations of KLAM_21 model characteristics. Left and centre: Universal vertical profiles of normalised temperature disturbance $T'/\Delta T$ and normalised horizontal wind velocity $v_h/<v_h>$. Dashed lines indicate H_{eff}/H. Right: Plain view of the Arakawa C grid structure for horizontal wind components u and v, the total heat deficit E, and the cold air layer depth H. i and j are grid cell indices in west-east and south-north directions.

The model is initialised with zero wind and neutral stratification at 1800 NZST (New Zealand Standard Time), which corresponds approximately with the onset time of nocturnal cooling. Integration over time is carried out on a regular Arakawa C grid (Figure 1) using dynamically calculated time steps to fulfil the Courant-Friedrich-Levy criterion. The size of the computational domain is *150 km x 140 km* with a horizontal resolution of *500 m* in the outer domain and *100 m* in the nested inner grid (see Figure 3). Spatial gradients are discretised using centred differential quotients. Advection of heat loss by the mean wind (eq. 1) is calculated with a donor-cell algorithm. For further details of KLAM_21 see Sievers (2005).

Table 1: Local heat loss rates P in KLAM_21.

Surface type	open country	shrubland	forest	urban	dense urban	lake, river	sea
P [W m^{-2}]	30.0	22.5	16.8	8.4	0.0	0.0	-6.0

3. OBSERVATIONS

The 50 μg m^{-3} 24h mean concentration health guideline for PM_{10} is exceeded in Christchurch about 30 times per winter on average (Spronken-Smith et al., 2002). The highest concentrations typically occur under calm synoptic conditions between sunset and midnight when emissions from domestic heating are highest and dispersion is strongly influenced by local winds and surface temperature inversions. Figure 2 shows observed surface winds in the Christchurch area about 3 h after sunset on 8 June 2000, which was a typical smog night during the CAPS2000 field campaign (Kossmann and Sturman 2004) with weak ambient winds and an observed 24h mean PM_{10} concentration of 83 μg m^{-3}. On the regional scale the surface wind field is characterised by drainage winds down the Canterbury Plains and land breezes along the coastline. Flow splitting is caused by the terrain elevations of the Port Hills and Banks Peninsula. Over the urban area of Christchurch northwesterly regional drainage winds down the Canterbury Plains converge with local southerly drainage winds from the Port Hills (Figure 2). This zone of flow convergence is characterised by very weak winds which favour the accumulation of air pollutants. Later in the night the regional scale northwesterly drainage winds become more dominant and the convergence zone is shifted southward towards the Port Hills (Corsmeier, 2006).

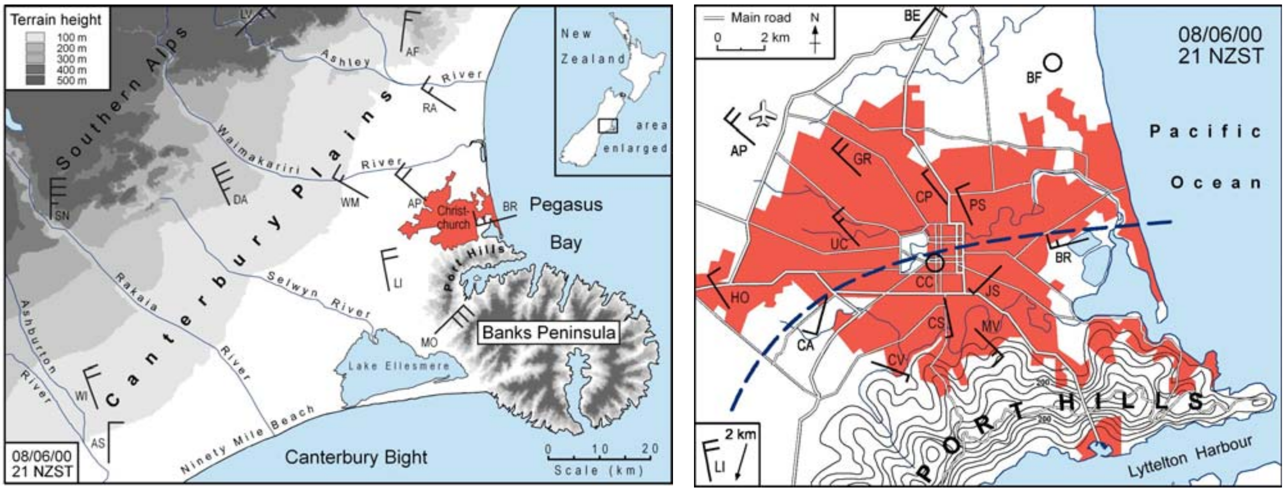

Figure 2: Topography of study area and observed surface winds on 8 June 2000, 2100 NZST. Long barbs indicate 1 m s^{-1} each, short barbs indicate 0.5 m s^{-1}, and open circles indicate calms. Left: Coastal Canterbury area. Right: Christchurch urban area. The dashed line illustrates the convergence zone of regional and local drainage winds.

4. MODEL RESULTS

Figure 3 shows KLAM_21 results of the regional surface wind field after 3 hours of simulation (2100 NZST). The structure and intensity of the main observed flow features, such as cold air drainage down the Canterbury Plains, flow splitting northeast of Banks Peninsula and land breezes along the coastlines are well captured by the model. The model also simulates the observed convergence of regional drainage winds down the Canterbury Plains and local drainage winds from the Port Hills, and the associated poor ventilation (low cold air volume fluxes) over the Christchurch urban area. The minimum in the modelled effective cold air layer depth over the city centre and the eastern suburbs represents the urban heat island, which causes the formation of country breezes which are superimposed on to drainage winds and land breezes (Figure 4).

REFERENCES

Corsmeier, U., M. Kossmann, N. Kalthoff, and A.P. Sturman, 2006: Temporal evolution of winter smog within a nocturnal boundary layer at Christchurch, New Zealand. *Meteor. Atmos. Phys.* **91**, 129-148.

Kossmann, M. and A.P. Sturman, 2004: The surface wind field during winter smog nights in Christchurch and coastal Canterbury, New Zealand. *Int. J. Climatology* **24**, 93-108.

Sievers, U., 2005: Das Kaltluft-Abfluss-Modell KLAM_21. Grundlagen, Anwendungen und Handhabung des PC-Modells. *Berichte des Deutschen Wetterdienstes* **127**. Deutscher Wetterdienst, Offenbach a.M., Germany, 101 pp.

Spronken-Smith, R.A., A.P. Sturman, and E.V. Wilton, 2002: The air pollution problem in Christchurch, New Zealand – progress and prospects. *Clean Air and Environmental Quality* **36**, 23-29.

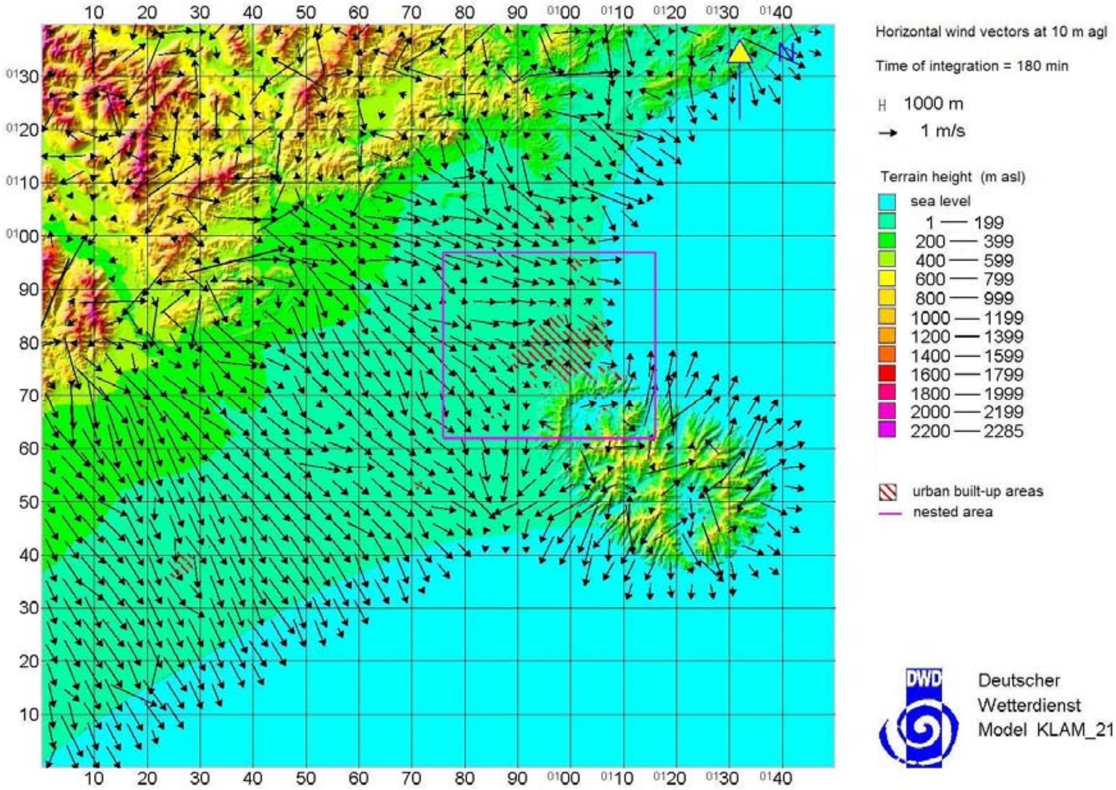

Figure 3: Computational domain of the KLAM_21 simulations. The nested area (*40 km x 35 km*) with higher spatial resolution is indicated by the rectangle around the area of Christchurch. Colour shading indicates terrain height above sea level. Arrows represent horizontal wind vectors at 10 m above ground level after 3h of simulation (2100 NZST). Wind vectors are only plotted at 4 km intervals for wind speeds exceeding 0.05 m s^{-1} and for $H > 10\ m$.

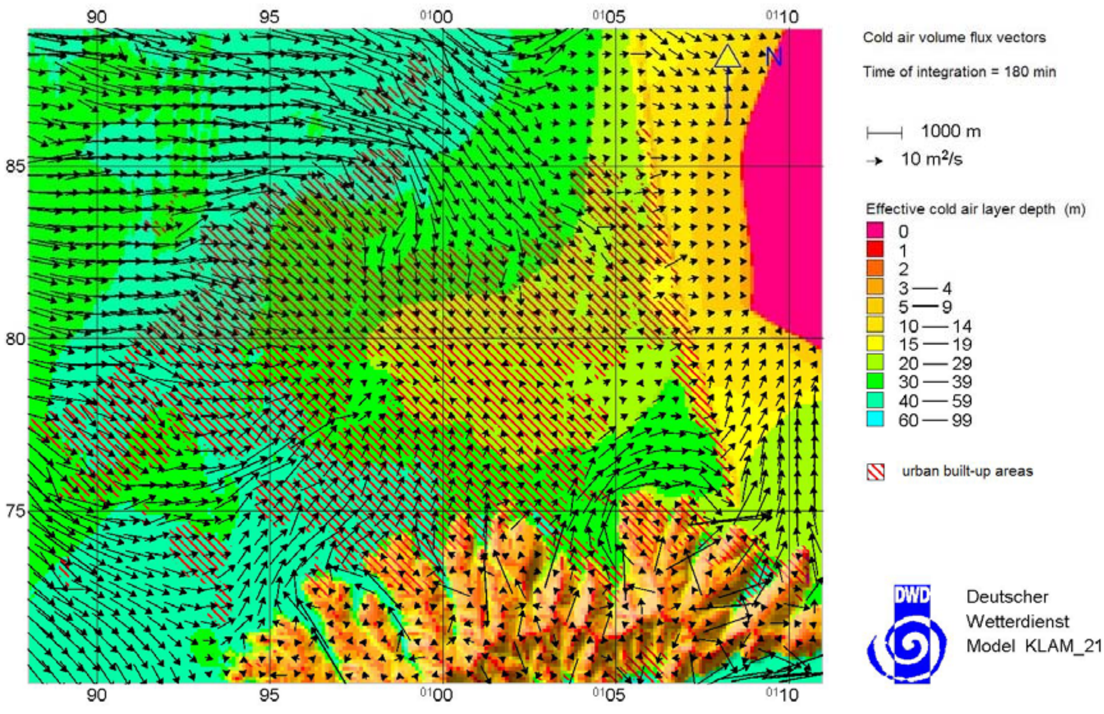

Figure 4: Vectors of the vertically integrated cold air flux (volume flux) and effective cold air layer depth H_{eff} over the Christchurch area after 3h of simulation (2100 NZST). The shape of the terrain elevation is indicated by sun shading superimposed on the colour shading of the effective cold air layer depth. Volume flux vectors are only plotted at 500 m intervals. Urban built-up areas are marked by red diagonal stripes.